JOURNAL OF APPLIED ELECTROCHEMISTRY 21 (1991) 848–857

The electrochemistry of Magnéli phase titanium oxide ceramic electrodes
Part I. The deposition and properties of metal coatings*

J. E. GRAVES, D. PLETCHER
Department of Chemistry, The University, Southampton SO9 5NH, Great Britain

R. L. CLARKE
Dextra Associates, 74 Muth Drive, Orinda, U.S.A.

F. C. WALSH
Chemistry Department, Portsmouth Polytechnic, Portsmouth PO1 2DT, Great Britain

Received 30 November 1990; revised 1 February 1991

The electrodeposition of copper, gold, nickel, palladium and platinum onto Ebonex® ceramic cathodes has been studied. It is demonstrated that good quality deposits may be obtained and that the kinetics of the deposition and dissolution of metals are similar at Ebonex® to other common substrates (for example, Pt, C). In addition, the kinetics of some simple redox couples at coated and bare Ebonex® ceramic electrodes are compared; it is confirmed that such electron transfer reactions are very slow on the bare Ebonex® ceramic but when the surface is coated with a metal, the kinetics are similar to those on the bulk metal.

1. Introduction

Ceramic materials have a growing importance in electrochemical technology. Usually, however, they are used in the form of coatings on a metal substrate; the best known examples are the ruthenium dioxide and iridium dioxide based coatings on titanium, now widely used as anodes for chlorine and oxygen evolution, respectively [1–3]. Other ceramic coatings would, however, include spinels [4–6] and tungsten bronzes [7]. Less commonly, ceramic materials have a conductivity high enough that they may be used as electrodes in the form of bulk materials. Thus, magnetite (Fe_3O_4) was, for many years, used as an anode in the chlor-alkali industry [8] and several papers have discussed the application of borides, carbides, nitrides etc. as electrocatalysts [9] and inert substrates for electron transfer [10–12] as well as tungsten bronzes [13]. Despite this considerable body of work, understanding of the electrochemical properties of conducting ceramics remains very limited. Indeed, there is commonly substantial disagreement over properties as fundamental as their stability to corrosion and the overpotentials for hydrogen and oxygen evolution as well as evidence that such properties can depend strongly on the method and conditions of preparation [14].

Ebonex®† is a conducting ceramic material mainly composed of the Magnéli phase titanium oxides, Ti_4O_7 and Ti_5O_9 [15–17]. It is prepared by the high temperature hydrogen reduction of titanium dioxide and has several properties which warrant its consideration as an electrode material. For example, it has a bulk conductivity of $10^3\,\Omega^{-1}\,cm^{-1}$, is resistant to corrosion in a wide range of media and shows no tendency to hydride in contact with hydrogen. Applications of Ebonex® as an electrode material have been covered by several patents [18, 19] and have also been discussed in recent reviews [15–17]. On the other hand, few papers describe laboratory studies of its fundamental electrochemistry. An early paper by Pollock *et al.* [20] reported high overpotentials for both hydrogen and oxygen evolution at Magnéli phase titanium oxide electrodes. More recently, a short note by Miller-Folk, Noftle and Pletcher [21] demonstrated that the kinetics of the ferro/ferricyanide couple were slow at an Ebonex® electrode although, in contrast, lead and palladium could be electrodeposited without significant overpotentials. It has also been shown that it is possible to electrodeposit PbO_2 onto Ebonex® and the properties of such electrodes have been reported [22].

This paper reports the extension of the study by Miller-Folk *et al.* [21] to the electrodeposition of other

* This paper is dedicated to Professor Dr Fritz Beck on the occasion of his 60th birthday.
† Ebonex® is a registered trademark of Ebonex Technologies Inc.

0021-891X/91 $03.00 + .12

metals and to the study of several redox couples at both bare and metal coated Ebonex®. It was considered important to base any conclusions about electron transfer at Ebonex® surfaces on the results from the investigation of several redox couples. Moreover, since the kinetics of electron transfer reactions could be strongly influenced by the formation of less conducting (more oxidized) titanium oxide layers on the surface, it was considered essential to study couples with different formal potentials. The couples selected were Ce(IV)/Ce(III) ($E_e^0 \approx +1.21$ V/SCE in 1 M H_2SO_4), $Fe(CN)_6^{4-}/Fe(CN)_6^{3-}$ ($E_e^0 \approx +0.24$ V/SCE) and $[Fe(III)EHPG]^-/[Fe(II)EHPG]^{2-}$ (EHPG is the ligand ethylenebis-(2-hydroxyphenylglycine), $E_e^0 \approx -0.58$ V/SCE). The study of the electrodeposition of metals has been extended to five metals and the redox couples have also been investigated at appropriate electroplated Ebonex® electrodes. Such coated Ebonex® electrodes are, of course, also of interest for electrocatalytic reactions and such work will be reported in later papers.

While this paper only considers the behaviour of bulk, monolithic Magnéli phase titanium oxides, it is of interest to note that other workers [23, 25], including Fritz Beck [23], have reported electrochemical reactions at titanium oxide coatings made conducting by *in situ* cathodic reduction. For example, the ceramic Ti/TiO_2 electrode appears to be an active surface for the rapid reduction of nitrobenzene [23]. The relationship between these two types of titanium oxide electrodes remains to be defined.

2. Experimental details

Ebonex® ceramic electrodes were constructed from 2 mm thick sheets supplied by Ebonex Technologies Inc. Discs of 5 mm diameter were cut from the sheets using a diamond tool and electrical contact was made to a copper wire using silver loaded epoxy cement (RS Components 552–652). The electrodes were then encapsulated into glass tubes using an epoxy resin (A24–100, Philip Harris Scientific). For the fabrication of rotating disc electrodes, the ceramic disc was mounted onto a stainless steel unit, designed to connect to an EG + G Parc (Model 616) Rotating Motor, and then sealed into a Teflon sheath. One face of the electrode, area 0.2 cm^2, was exposed by grinding away the epoxy resin on silicon carbide paper.

Between experiments the surface of the Ebonex® electrodes were abraded with three grades of silicon carbide paper (p400A, p600A and p1200A) and/or polished with 0.3 and 0.05 μm alumina powder (Banner Scientific Co.) on a polishing cloth. The electrodes were then thoroughly washed with distilled water. For the other electrode materials polishing with alumina powder was found to be satisfactory.

Voltammograms were recorded using a Hi-Tek Instruments potentiostat (model DT 2101) and a function generator (model PPR1) with a Gould (model 60000) X–Y recorder. During constant current plating, a Fluke Digital Multimeter (model 8050A) was used to monitor the voltage of the working electrode: charges were measured with a workshop built coulometer. Measurements of pH were made with a B.D.H. pH electrode (309/1010).

All experiments were carried out in a three electrode, two compartment cell. The counter electrode was a platinum ring or spiral and the saturated calomel electrode was mounted in a separate compartment connected to the working electrode via a Luggin capillary.

All solutions were prepared from triply distilled water and high quality chemicals. The complex iron(III) ethylenebis-(2-hydroxyphenylglycine) was prepared as described in [26]. All solutions were degassed with a fast stream of nitrogen before any experiment was commenced.

The scanning electron micrographs were recorded using either (i) a Cambridge Stereoscan 150 SEM with an accelerating voltage of 20 kV and a beam current of 0.4 mA or (ii) a Jeol 35C SEM equipped with a Link model 860–500 energy dispersive X-ray analyser (EDAX) with an accelerating voltage of 27 kV and a beam current of 1 mA. For the plated cross section, the sample was mounted in epoxy resin and metallographically polished to leave a surface roughness of less than 0.1 μm.

The X-ray diffraction data was obtained on station 7.4 at the Synchrotron Radiation Source (SRS), SERC Daresbury Laboratory. The sample was a static, flat plate. A beam energy of 2 GeV and a beam current of 190 mA were employed. A Si (2 2 0) channel cut monochromator gave a beam wavelength of 0.142 nm at an incident angle of 4°. Data acquisition time was $\approx$ 600 s using an Inel 120° curved, position sensitive detector (3300 channels). Calibration was via silicon powder.

3. Results

3.1. *Characterization of the Ebonex® samples*

Ebonex® is available in several forms and porosities (determined by density measurements) but the electrodes in this study were manufactured from "non-porous" 2 mm thick sheet. The material is extremely robust and can be handled quite roughly without damage; it may, however, be cut and machined using ceramic workshop techniques and its surface may be abraided with silicon carbide paper and/or polished using polishing cloth methods. The conductivity of all samples employed were greater than $10^3 \Omega^{-1} cm^{-1}$.

Figure 1 shows a scanning electron micrograph of the surface of a sample of Ebonex® sheet. It can be seen that it is microrough and, despite the sample being termed "non-porous", that there are many, small pores. The Ebonex® was also examined by X-ray diffraction. A large number (> 30) of well resolved peaks were observed in the range $15° < 2\theta < 70°$. A complete analysis was not attempted but the peaks characteristic of Ti_4O_7 and Ti_5O_9, as reported by Goldschmidt and Watanabe [27], were

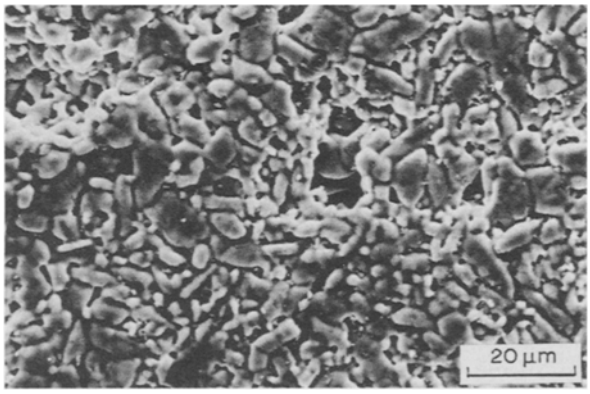

Fig. 1. Scanning electron micrograph of a "non-porous" Ebonex® sheet.

major features and it appeared that other titanium oxides were present as minor components.

When a sample of Ebonex® was subjected to anodic oxidation at very positive potentials in 1 M sulphuric acid (in fact, using a current density of 0.11 A cm^{-2} for 900 s), it gave an X-ray diffractogram which was markedly different; the amount of Ti_4O_7 had decreased substantially and higher oxides, including TiO_2, predominated. Variation of the angle of incidence showed that the composition was a function of depth from the surface. At even higher current density, a white film appears on the surface. These are, however, extreme treatments of the surface. Ebonex® anodes intended for oxygen evolution are normally prepared from high surface area materials (typically with 25% porosity) and the manufacturers recommend a lower current density ($\sim 20\,mA\,cm^{-2}$) so that the potential will remain much lower. Indeed polarization curves for Ebonex® show a limiting current for oxygen evolution whose magnitude depends strongly on the porosity of the sample; at the non porous material, the plateau current density is about $4\,mA\,cm^{-2}$.

The Ebonex® was also examined by cyclic voltammetry in acid, base and neutral aqueous solutions. These experiments are illustrated in Fig. 2 by two voltammograms recorded in 1 M H_2SO_4 with a potential scan rate of $50\,mV\,s^{-1}$. Figure 2a shows a 1st scan cyclic voltammogram initiated from 0.0 V and scanned first to negative potentials; a well formed but drawn out reduction wave is observed at $E_{1/2} = -0.45$ V/SCE and the equivalent oxidation charge is seen as a poorly formed and broad anodic peak around −0.53 V. This response seems to indicate reduction of the Ebonex® surface and reoxidation during the reverse scan but the processes certainly never gave sharp peaks such as those reported for the ceramic TiO_2 electrode by Beck and Gabriel [23]. Hydrogen evolution commences at −0.75 V/SCE. As the scan is continued to positive potentials it can be seen that, on this first sweep, there is an anodic current at all potentials. On the other hand, there are no peaks or waves prior to oxygen evolution which commences at +2.2 V. On the scan back to 0.0 V, no significant current is observed. Figure 2b shows the 2nd scan at this

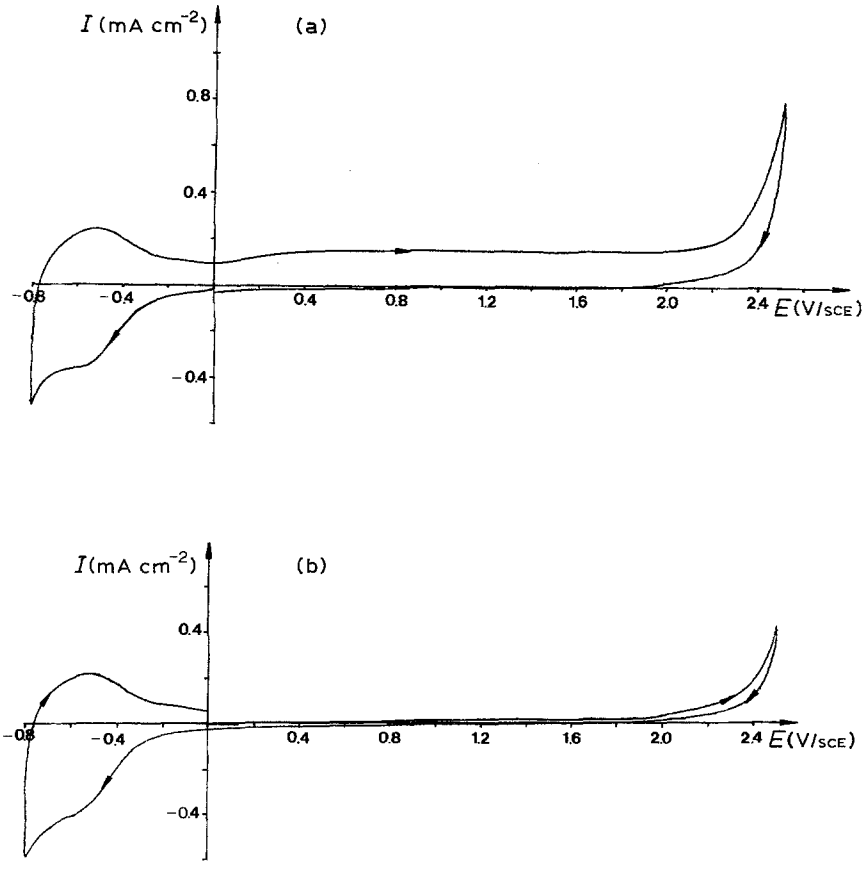

Fig. 2. Cyclic voltammograms recorded at $50\,mV\,s^{-1}$ for Ebonex® in 1 M sulphuric acid (a) 1st scan commencing at 0.0 V to negative potentials (b) 2nd scan commencing at 0.0 V to positive potentials. $T = 298$ K.

Ebonex® surface; in this experiment the scan is initially to positive potentials. The current density is much reduced compared to the first scan but is similarly featureless. At negative potentials, the response remains similar to the first scan. It would appear that the as-prepared Ebonex® surface has undergone irreversible oxidation during the first excursion to positive potentials although this change has surprisingly little effect to the processes at negative potentials. If the voltammetry is restricted to a lower positive potential limit, the difference between 1st and subsequent scans is less marked although the trend remains the same. Such voltammograms are not capable of detailed interpretation, particularly since the contribution of charging current to the response is likely to be substantial for this high area surface. Even so, it is clear that the surface layer(s) of the Ebonex® undergo slow and continuous changes in oxidation state over most of the potential range between hydrogen and oxygen evolution, at least until it is passivated.

3.2. *The electrodeposition of copper*

Figure 3 shows cyclic voltammograms recorded at Ebonex® and vitreous carbon disc electrodes in a commercial copper electroplating bath (composition shown in Table 1) using a potential scan rate of $100\,mV\,s^{-1}$. It can be seen that the curves have the same general shape and that the deposition and dissolution peaks occur at similar potentials; indeed, in both cases the reduction peak is observed at $-0.42\,V$/SCE. Hence, there is clearly no evidence that the reduction of copper(II) is inhibited at the Ebonex® electrode. The major difference between the curves is the magnitude of the dissolution peak and at Ebonex®, the stripping efficiency is only 20%. Moreover, oxidation current continues to be observed at potentials positive to the peak. Such "tailing", as well as the low stripping efficiency implies that much of the copper is deposited within the pores of the Ebonex® and is not readily accessible for rapid dissolution. This interpretation is confirmed by experiments at much slower scan rates when the stripping efficiency becomes larger as the quantity of copper deposited is increased.

The simplicity of the copper deposition reaction at Ebonex® is confirmed by RDE experiments with a solution containing 10 mM Cu^{2+} in 0.5 M Na_2SO_4, pH 2. The *I–E* curves at four rotation rates are reported in Fig. 4; well formed reduction waves are observed and the plateau currents are proportional to the square root of the rotation rate. The value of the diffusion coefficient for copper(II) estimated from the linear I_L against $\omega^{1/2}$ plot is $6.5 \times 10^{-6}\,cm^2\,s^{-1}$, identical to that obtained with a vitreous carbon disc.

Figure 5 shows scanning electron micrographs for copper deposits. Figure 5a shows a thin deposit, average thickness 1 μm when the copper can be seen as crystallites within the pores and surface unevenness. Figure 5b shows the surface of a much thicker deposit, thickness 50 μm, when the layer is complete and has an appearance typical of copper on other substrates. The final micrograph, Fig. 5c, shows a cross section of a thick deposit; this confirms the uniformity of the deposit. Energy dispersive X-ray analysis of the cross section clearly shows the presence of copper within the Ebonex® and it appears that the deposition occurs well down the pores within the material. The thick deposits appear to be mechanically stable and it requires vigorous abrasion to remove them. The microrough and microporous surface of the Ebonex® provides an excellent substrate for good adhesion.

3.3. *The electrodeposition of other metals*

Cyclic voltammograms were recorded at both Ebonex® and vitreous carbon electrodes for the gold, nickel,

Table 1. Conditions used for plating the metals on to Ebonex®. All depositions were carried out at 298 K.

Metal	*Plating solution*	*Plating control*	*Average thickness*
Cu	$75\,g\,dm^{-3}$ copper sulphate 2.2 M H_2SO_4 $50\,mg\,dm^{-3}$ Cl^- $1\,g\,dm^{-3}$ polyethylene-glycol $6\,mg\,dm^{-3}$ DS4	$I = 10\,mA\,cm^{-2}$	1–100 μm
Au	$8.2\,g\,dm^{-3}$ Au as $KAu(CN)_2$ $25\,g\,dm^{-3}$ citric acid, NH_3, pH 4.	$I = 1\,mA\,cm^{-2}$	0.1–20 μm
Ni	$300\,g\,dm^{-3}$ nickel sulphate $35\,g\,dm^{-3}$ nickel chloride $40\,g\,dm^{-3}$ boric acid H_2SO_4, pH 3.5	$I = 20\,mA\,cm^{-2}$	100 μm
Pd	10 mM palladium chloride 1 M potassium chloride HCl, pH 3	$E = -50\,mV$/SCE	1–5 μm
Pt	10 mM chloroplatinic acid 1 M hydrochloric acid	$E = -200\,mV$/SCE	1–3 μm

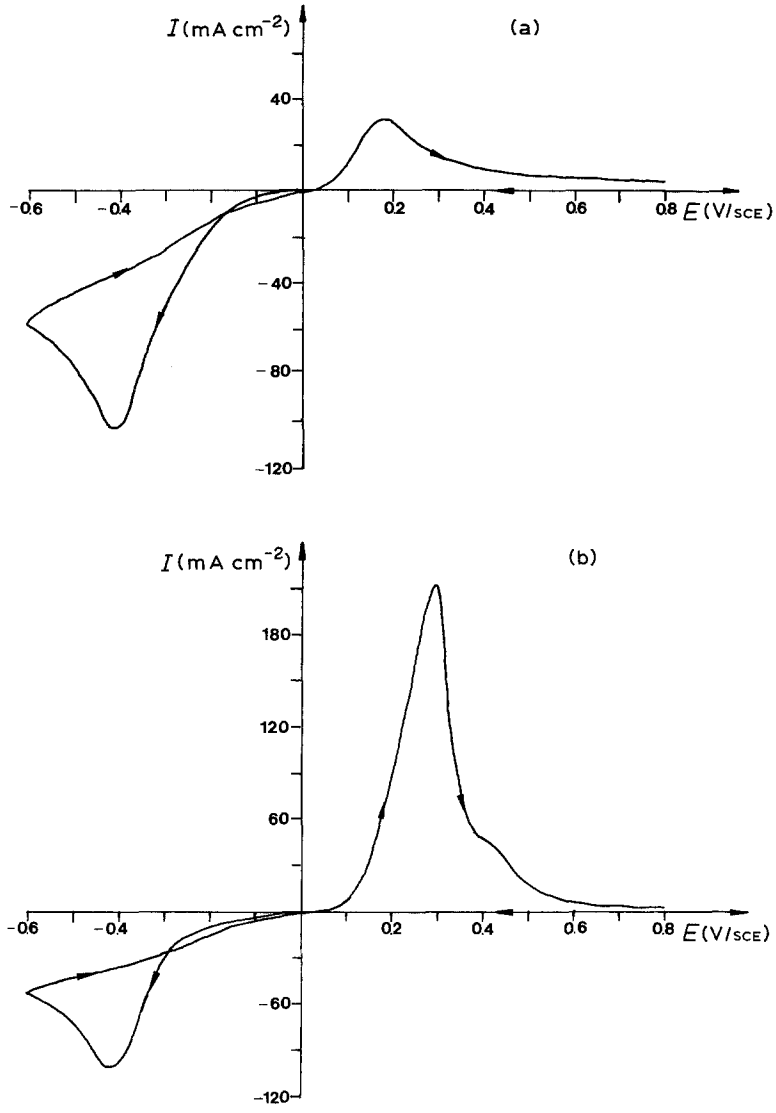

Fig. 3. Cyclic voltammograms recorded at (a) Ebonex® and (b) vitreous carbon electrodes in a commercial copper plating bath. Potential scan rate 100 mV s^{-1}. T = 298 K.

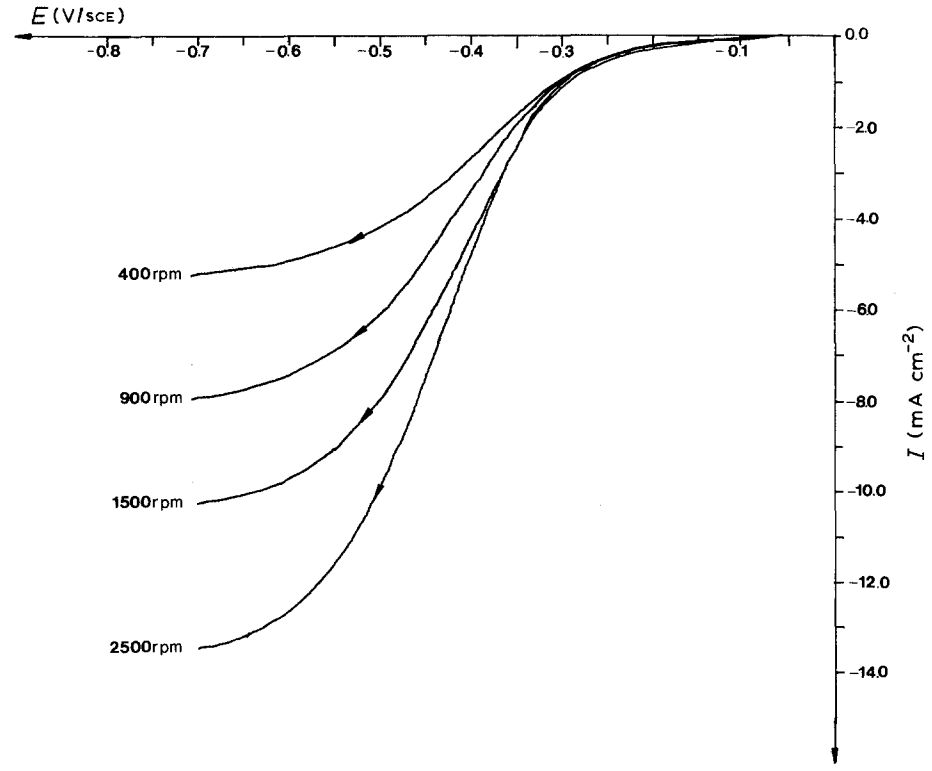

Fig. 4. I–E characteristics as a function of rotation rate for Ebonex® in a solution of copper(II) sulphate (10 mM), sodium sulphate (0·5 M), pH 2. Potential sweep rate 5 mV s^{-1}. T = 298 K.

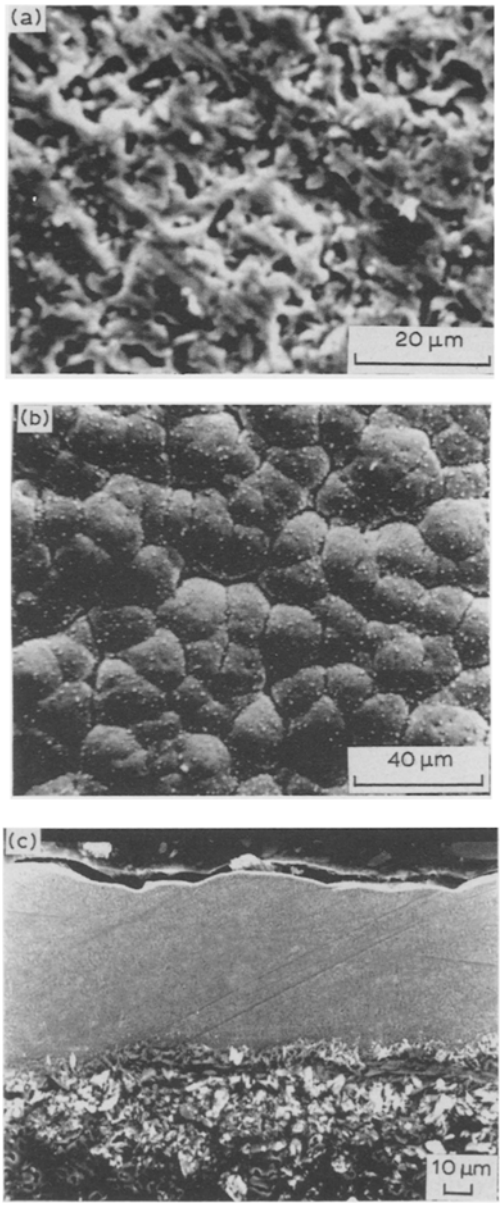

Fig. 5. Scanning electron micrographs for copper deposits: (a) thin deposit, average thickness 1 μm; (b) thicker deposit, average thickness 50 μm; and (c) cross section of a thick deposit.

palladium and platinum electroplating solutions listed in Table 1. The voltammograms for each metal ion are again very similar at both vitreous carbon and Ebonex® and there certainly does not appear to be any special barrier to electron transfer at the Ebonex® surface. On the other hand, the voltammograms for the four metals ions are, of course, quite different; for example (a) the deposition of the metals occurs at markedly different potentials (+0.2 V for Pt, −1.0 V for Ni) where the Ebonex® surface might be expected to have different properties, (b) the overpotentials associated with both deposition and dissolution depend strongly on the metal and (c) Pd shows facile dissolution while Pt does not show an anodic stripping peak.

Electroplated Ebonex® electrodes were prepared in the conditions listed in Table 1. The thicker electrodeposits (Ni and Cu) were reflective and all appeared to adhere well. Certainly the deposits could be used as electrodes in laboratory conditions for an extended period of time. The precious metals were deposited only as thin layers and electron microscopy showed that these were not continuous. Rather, individual crystals of the metals could be seen distributed over the microrough surface of the Ebonex®. The high area of the deposits could be confirmed by cyclic voltammetry in 1 M sulphuric acid. For example, a Pt deposit averaging 2.4 μm in thickness gives a voltammogram with the characteristic two adsorption and two desorption peaks for hydrogen but the charge associated with the processes is 75 mC cm^{-2}.

3.4. *The kinetics of redox processes at bare and coated Ebonex®*

Figure 6 shows a series of cyclic voltammograms for 5 mM [Fe(III)EHPG]$^-$ in 1 M aqueous sodium acetate at copper, Ebonex® and Ebonex® electroplated with 10 μm copper. At copper, Fig. 6a, the [Fe(III)EHPG]$^-$/[Fe(II)EHPG]$^{2-}$ couple has the characteristics of a quasi-reversible electron transfer process; well formed reduction and coupled oxidation peaks are observed around −0.62 V but the peak separations are greater than 60 mV (90–130 mV with the scan rates shown). The value of the diffusion coefficient estimated from the slope of the linear I_p^C against $v^{1/2}$ plot is 4×10^{-6} cm^2 s^{-1}. On Ebonex®, Fig. 6b, the response is quite different. The current function for the reduction process is the same as at copper but the reduction peak is shifted to much more negative potentials, around −0.9 V and the process becomes irreversible. Only a small and drawn out oxidation peak is observed at about −0.40 V/SCE on the reverse scan. Once the Ebonex® has been plated with copper, however, the response returns to that at the bulk copper, Fig. 6c.

The story of the ferricyanide/ferrocyanide couple in 1 M potassium chloride at platinum, Ebonex® and Ebonex® plated with 2.4 μm platinum is similar and single voltammograms for ferricyanide at each surface is shown Fig. 7. The couple is reversible at both platinum and the platinum coated ceramic. In contrast at Ebonex® both the reduction and oxidation processes require an overpotential which is a function of the history of the Ebonex® surface; oxidation of the surface increases the overpotentials for electron transfer, see Fig. 7d and [21]. The influence of the surface oxidation on the kinetics of the oxidation reaction is also clearly seen on a RDE. While the rotation rate dependence of the reduction wave for ferricyanide is quite normal (although the waves are displaced to around −0.6 V/SCE), the curves for the oxidation of ferrocyanide do not show well formed plateaux and the current densities are never stable, decreasing slowly for long periods of time.

The Ce(IV)/Ce(III) couple in sulphuric acid was also studied at both bare and Pt plated Ebonex®. At a RDE prepared from bare Ebonex®, Ce(IV) gave simple, well formed reduction waves at each rotation rate but not until $E_{1/2} \approx -50$ mV, an overpotential of > 1.25 V, see Fig. 8a. On the other hand, it was not

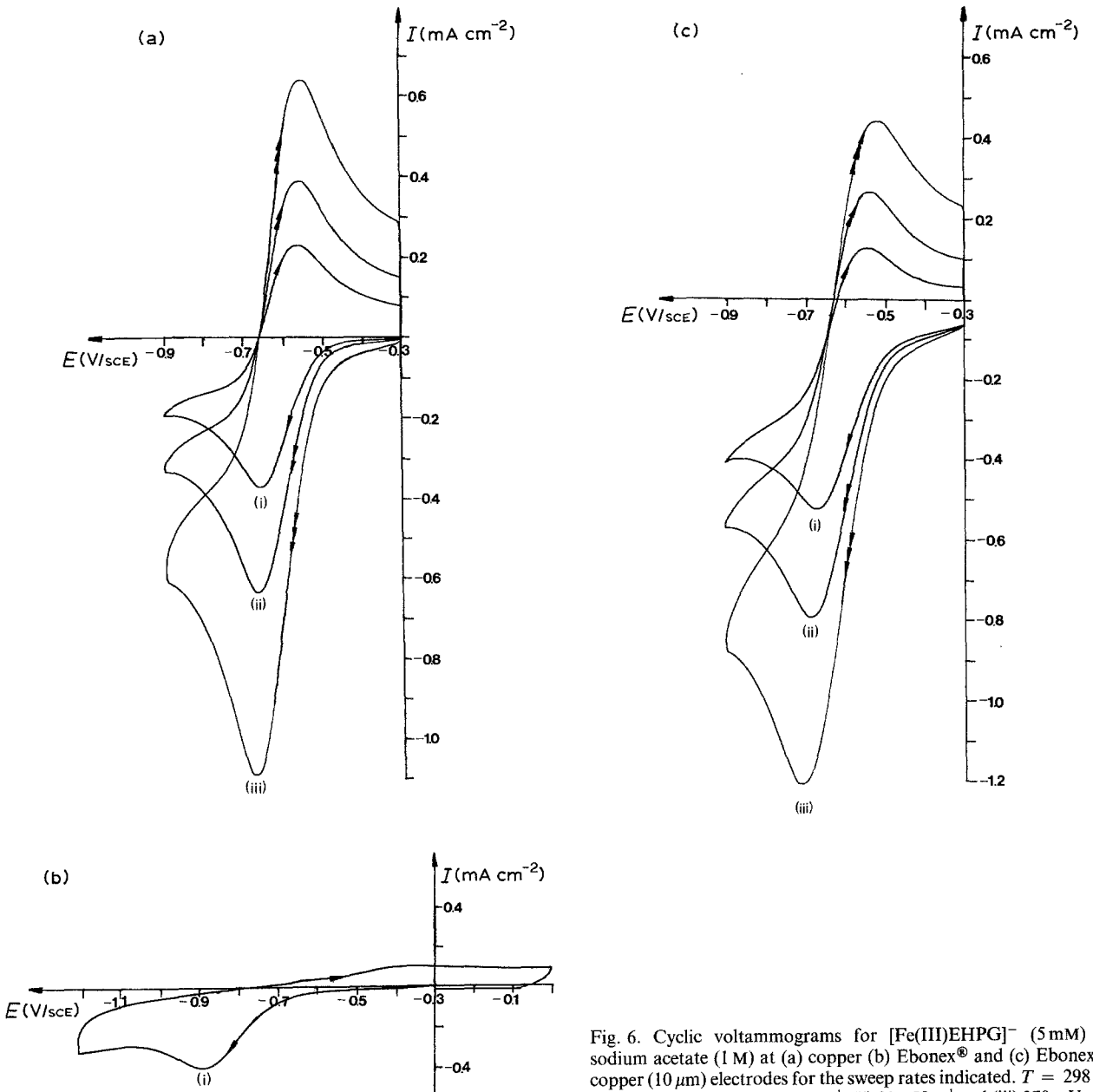

Fig. 6. Cyclic voltammograms for $[Fe(III)EHPG]^-$ (5 mM) in sodium acetate (1 M) at (a) copper (b) Ebonex® and (c) Ebonex®/copper (10 μm) electrodes for the sweep rates indicated. T = 298 K. Potential scan rates (i) 30 mV s^{-1}, (ii) 90 mV s^{-1} and (iii) 270 mV s^{-1}.

possible to observe oxidation of Ce(III) before oxygen evolution although even on Pt, the anodic oxidation of Ce(III) occurs only just prior to O_2 evolution; figure 8b shows the I–E curve for the Ce(III) solution and it is identical to that for H_2SO_4 alone. Once Pt plated, however, the Ebonex® electrode gave an I–E curve for a solution containing both Ce(III) and Ce(IV) with a single wave crossing the zero current axis at +1.20 V and with good oxidation and reduction limiting current plateaux which were mass transport controlled, i.e. the couple has rapid kinetics.

4. Discussion

The results show clearly that metals may be electroplated onto Ebonex® to give good quality, adhesive deposits. Indeed, Ebonex® may have a surface morphology (microrough and porous) which give it particularly good properties as a substrate for metal layers. With low loadings of metal, high surface area deposits are obtained but as the layer thickness its surface morphlogy probably depends on the metal being plated as well as the bath being used. Certainly, in the case of copper from the commercial acid plating bath, the surface becomes very uniform.

The cyclic voltammograms of the Ebonex® in sulphuric acid (and, indeed, other aqueous electrolytes) show no well defined peaks which may be attributed to particular changes in the oxidation state of the titanium in the surface. On the other hand, particularly during the first scan in potential sweep experiments, there are substantial "background" currents at all potentials and while there will be some contribution from charging current at the high area Ebonex®, it is probable that most of the charge passed leads to oxidation/reduction of the surface. It seems likely that the titanium in the surface layer(s) undergo continuous changes in oxidation state as the potential is made

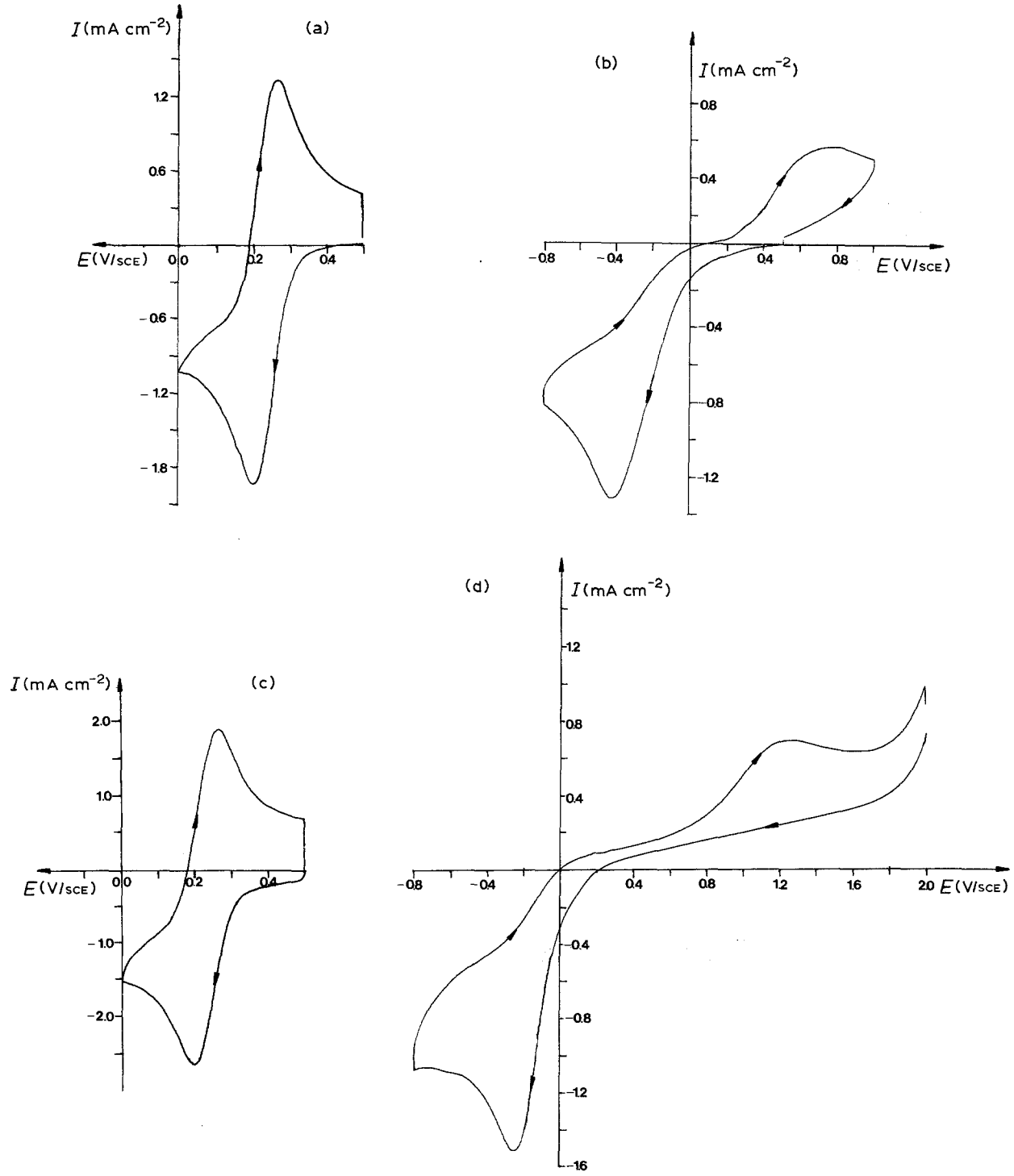

Fig. 7. Cyclic voltammograms recorded at 100 mV s^{-1} for potassium ferricyanide (10 mM) in potassium chloride (1 M) at (a) platinum (b) Ebonex® (c) Ebonex®/platinum (2.4 μm) and (d) oxidized Ebonex® electrodes. T = 298 K.

more positive. Certainly, in very forcing conditions at high potentials, the X-ray diffraction data show conclusively that oxidation has occurred and TiO_2 has been formed on the surface of the Ebonex®. Such oxidation of of the Ebonex® appears to be inhibited when the surface is coated with PbO_2 [28].

The kinetics of three couples were studied at bare Ebonex® and the results are summarized in Table 2. We would stress the following features of the results:
(a) with the $Fe(CN)_6^{3-}/Fe(CN)_6^{4-}$ and $[Fe(III)EHPG]^-/[Fe(II)EHPG]^{2-}$ couples both oxidation of the reduced species and reduction of the oxidized species in solution occurs although all reactions require a substantial overpotential. In contrast, the kinetics of the couples are rapid when the Ebonex® is electroplated with a suitable metal.
(b) oxidizing the Ebonex® surface further, reduces the rate of oxidation of ferrocyanide.
(c) the data for the Ce(IV)/Ce(III) couple at Ebonex® is difficult to assess because oxygen evolution prevents any reasonable chance of observing the oxidation of Ce(III). It is, however, clear that the reduction of Ce(IV) requires a very large overpotential.
(d) the data for all three couples should be interpreted

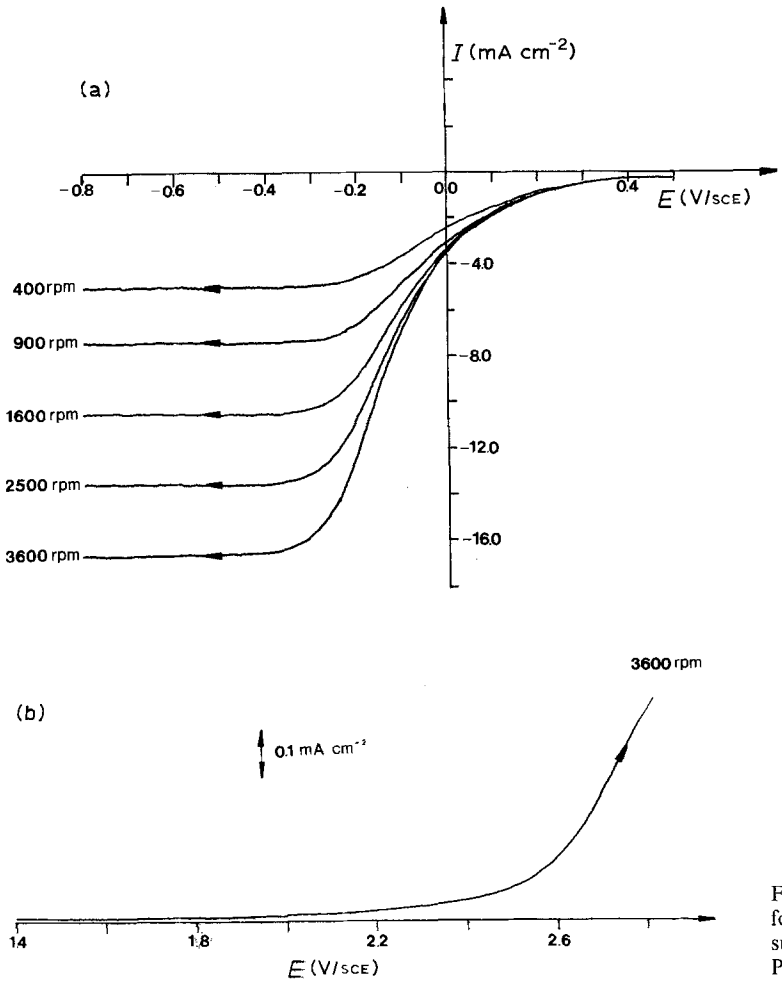

Fig. 8. *I–E* characteristics as a function of rotation rate for Ebonex® in a solution of cerium(IV)/cerium(III) sulphate (25 mM each) in sulphuric acid (0.5 M). Potential sweep rate 2 mV s^{-1}. T = 298 K.

as showing that the overpotential for any electron transfer process increases as its formal potential becomes more positive, i.e. as the surface becomes more oxidized, electron transfer becomes more difficult. Indeed, we have found no evidence for oxidation/reduction of redox species positive to +1 V.

(e) On the other hand, both oxidation and reduction can be observed at bare Ebonex®, e.g. the $Fe(CN)_6^{3-}$/$Fe(CN)_6^{4-}$ and $[Fe(III)EHPG]^-$/$[Fe(II)EHPG]^{2-}$ couples. Moreover, in comparison to the behaviour of redox couples at TiO_2 coated Ti electrodes [29], the magnitudes of the overpotentials for oxidation and reduction are of a similar magnitude. The TiO_2 coated Ti surface shows classical semi-conductor behaviour and this is not the case for Ebonex®. It is interesting to note, however, that the paper by Schultze *et al.* [29] did report that plating the TiO_2 with gold led to a surface again able to support rapid kinetics for the $Fe(CN)_6^{3-}$/$Fe(CN)_6^{4-}$ couple.

(f) even if electron transfer is inhibited by surface oxidation at positive potentials, the contrast between the redox couples and metal deposition reactions in the potential range +0.3 V to −1.2 V remains. The redox couples require a substantial overpotential while metal deposition reactions do not. It is also true that PbO_2 may be deposited anodically without an unusually high overpotential [28].

The properties of the surface leading to inhibition of the kinetics of redox couples is not clear. For example, if (a) the surface layer were to act as a semi-conductor, either oxidation or reduction of species in solution would be inhibited to a much greater extent than the other or (b) the surface layer had a high resistance, the whole *I–E* response would be expected to be

Table 2. Summary of the voltammetric data for the redox couples at bare and electroplated Ebonex® electrodes

Couple	E_e^0 (*V*/SCE)	*Ebonex®*			*Plated Ebonex®*	
		E_p^C (*V*/SCE)	E_p^A (*V*/SCE)	ΔE_p (*mV*)	*Metal*	ΔE_p (*mV*)
$[Fe(III)EHPG]^-$/ $[Fe(II)EHPG]^{2-}$	−0.58	−0.90	−0.38	520	Cu	90
$Fe(CN)_6^{3-}$/$Fe(CN)_6^{4-}$	+0.24	−0.40	+0.56	960	Pt	60
Ce(IV)/Ce(III)	+1.21	−0.15	–	–	Pt	75

distorted. It should also be noted that slow kinetics for solution-free redox couples is not a general property of all conducting ceramics; rapid kinetics have been reported for the $Fe(CN)_6^{3-}/Fe(CN)_6^{4-}$ and other couples have been reported for several ceramic electrodes [11, 13].

Perhaps, not surprisingly, the coated Ebonex® electrodes have properties which are dominated by those of the plated metal. In particular, it has been shown that redox couples can have very rapid kinetics at the coated electrodes and this is in complete contrast to the bare Ebonex® where the oxidation and reduction of redox species in solution is inhibited. This observation does, however, confirm that the surface layers of the Ebonex® do not simply behave as a resistance since such a barrier would then influence the properties of the coated electrodes.

It is also interesting to consider the early stages of metal deposition onto the Ebonex® surface. It should be recognised that much of the thickening of the metal layer as well as the dissolution process occurs under conditions where the interface is between the metal and the solution. It is, therefore, only the initial stage of metal deposition which is the puzzle – How can ions in solution be reduced at low overpotential when the reaction leads to metal but not if the process leads to another species in solution? It is only possible to speculate but perhaps the metal atoms become incorporated into the titanium oxide surface leading to changes in its properties. A similar mechanism may pertain during the electrodeposition of PbO_2 although this reaction occurs at quite positive potentials. The difference between phase formation and redox reactions is certainly striking and deserves further study.

From a technological viewpoint, uncoated Ebonex® electrodes are likely only to find application when it is advantageous to avoid conversion of redox species in solution [19]. On the other hand, Ebonex® could be an excellent substrate for metals and other catalysts (for example, PbO_2) and it would be interesting to carry out some long term testing of electroplated Ebonex® materials as electrodes for regenerating solutions of redox reagents.

Acknowledgement

The authors would like to thank Ebonex Technologies Inc for financial support of this work.

References

[1] P. Schmittinger, L. C. Curlin, T. Asawa, S. Kotowski, B. B. Beer, A. M. Greenberg, E. Zelfel and R. Breitstrade in 'Ullmann's Encyclopedia of Industrial Chemistry', Vol. 6A, 5th edition, VCH Verlag, Weinheim (1986).
[2] D. Pletcher and F. C. Walsh, 'Industrial Electrochemistry', 2nd edition, Chapman and Hall, London (1990).
[3] A. M. Couper, D. Pletcher and F. C. Walsh, *Chem. Reviews* **90** (1990) 837.
[4] M. R. Tarasevich and B. M. Efremov in 'Electrodes of Conductive Metal Oxides, Part A' (edited by S. Trasatti), p. 221, Elsevier, Amsterdam (1984).
[5] W. J. King and A. C. C. Tseung, *Electrochim. Acta* **19** (1974) 485.
[6] S. Trasatti, *Materials Chem. and Phys.* **16** (1987) 157.
[7] D. B. Sepa, A. Damjanovic and J. O'M. Bockris, *Electrochim. Acta* **12** (1967) 746.
[8] A. T. Kuhn in 'Industrial Electrochemical Processes', (edited by A. T. Kuhn), p. 533, Elsevier, Amsterdam (1971).
[9] J. P. Randin in 'Comprehensive Treatise of Electrochemistry', Vol. 4 (edited by J. O'M. Bockris, B. E. Conway, E. Yeager and R. White), p. 473, Plenum Press, New York (1982).
[10] F. Mazza and S. Trasatti, *J. Electrochem. Soc.* **110** (1963) 847.
[11] E. Pungor and A. Weser, *Anal. Chem. Acta* **47** (1969) 147.
[12] S. Meguro, B. Ise and O. Takagi, *Kinzoku Hyomen Gitutsu* (1986) 37.
[13] M. Amjad and D. Pletcher, *J. Electroanal. Chem.* **59** (1975) 61.
[14] R. D. Armstrong and M. F. Bell, *Electrochim. Acta* **23** (1978) 1111.
[15] R. L. Clarke in 'Proceedings of the Second International Forum on Electrolysis in the Chemical Industry', Deerfield Beach, Florida (1988).
[16] P. C. S. Hayfield and R. L. Clarke in 'Proceedings of the Electrochemical Society Meeting', Los Angeles (1989).
[17] R. L. Clarke and S. K. Harnsberger, *Am. Lab.* **20**(6A) (1988) 6.
[18] P. C. S. Hayfield, US Patent 4422917 (1983).
[19] N. L. Weinberg, J. D. Genders and R. L. Clarke, US Patent 4936970 (1990).
[20] R. J. Pollock, J. F. Houlihan, A. N. Bain and B. S. Coryea, *Materials Res. Bull.* **19** (1984) 17.
[21] R. R. Miller-Folk, R. E. Noftle and D. Pletcher, *J. Electroanal. Chem.* **274** (1989) 257.
[22] M. Mayr, W. Blatt, B. Busse and H. Heinke in 'Proceedings of the Fourth International Forum on Elecrolysis in the Chemical Industry', Fort Lauderdale, Florida (1990).
[23] F. Beck and W. Gabriel, *Angew. Chem. Int. Ed.* **24** (1985) 771.
[24] S. Muralidharan, C. Ravichandran, S. Chellammal, S. Thangavelu and P. N. Anantharam, *Bull. Electrochem.* **5** (1989) 533.
[25] D. Laser, M. Yaniv and S. Gottesfeld, *J. Electrochem. Soc.* **125** (1978) 358.
[26] R. B. Lauffer, W. L. Greif, D. D. Stark, A. C. Vincent, S. Saini, V. J. Wedeen and T. J. Brady, *J. Comp. Assist. Tomography* **9** (1985) 431.
[27] D. Goldschmidt and M. Watanabe, *Materials Res. Bull.* **20** (1985) 65.
[28] R. L. Clarke, unpublished data.
[29] J. W. Schultze and C. Bartels, *J. Electroanal. Chem.* **150** (1983) 583.